ELSEVIER

Contents lists available at ScienceDirect

Ad Hoc Networks

journal homepage: www.elsevier.com/locate/adhoc





An in-depth assessment of the physical layer performance in the proposed B5G framework

Juan Diego Belesaca ^a, Andres Vazquez-Rodas ^{a,*}, Luis F. Urquiza-Aguiar ^b, J. David Vega-Sánchez ^c

- a Department of Electrical Engineering, Electronics and Telecommunications, Universidad de Cuenca, Cuenca, 010101, Azuay, Ecuador
- ^b Departamento de Electrónica, Telecomunicaciones y Redes de Información, Escuela Politécnica Nacional, Quito, Pichincha, Ecuador
- c Faculty of Engineering and Applied Sciences (FICA), Telecommunications Engineering, Universidad de Las Américas (UDLA), Quito 170124, Ecuador

ARTICLE INFO

Keywords: 5G NR PDSCH Clustered delay line Tapped delay line Channel estimation Synchronization Convolutional neural network Beyond 5G

ABSTRACT

The introduction of fifth-generation (5G) technology marks a significant milestone in next-generation networks, offering higher data rates and new services. Achieving optimal performance in 5G and beyond 5G (B5G) systems requires addressing key requirements like increased capacity, high efficiency, improved performance, low latency, support for many connections, and quality of service. It is well-known that suboptimal network configuration, hardware impairments, or malfunctioning components can degrade system performance. The physical layer of the radio access network, particularly channel estimation and synchronization, plays a crucial role. Hence, this paper offers an in-depth evaluation of the 5G Physical Downlink Shared Channel (PDSCH), along with its related channel models such as the Clustered Delay Line (CDL) and the Tapped Delay Line (TDL). This work assesses 5G network performance through practical and IA-based channel estimation and synchronization techniques, and anticipates numerologies for B5G networks. Extensive simulations leveraging the Matlab 5G New Radio (NR) toolbox assess standardized channel scenarios in both macro-urban and indoor environments, following configurations set by the 3rd Generation Partnership Project (3GPP). The numerical results offer valuable insights into achieving the maximum achievable throughput across various channel environments, including both line-of-sight (LoS) and non-line-of-sight (NLoS) conditions. The throughput comparisons are performed under assumptions of ideal, realistic, and convolutional neural networks (CNN)based channel estimation with both perfect and realistic synchronization conditions. Importantly, the study pinpoints certain physical layer elements that have a pronounced impact on system performance, providing essential insights for devising effective strategies or refining CNN-based methods for forthcoming mobile B5G networks.

1. Introduction

The transition from 4G to 5G faces challenges due to compatibility issues between 4G base stations (BSs) and 5G New Radio (NR) specifications. Phase 1 of 5G, non-standalone (NSA) 5G, transforms existing 4G networks incrementally to reduce costs and risks, whereas Phase 2 requires a complete re-inspection of the current 4G network infrastructure and significant financial investment to realize 5G. This gradual transition is expected to continue from the 5G to Beyond 5G (B5G) and 6G networks [1].

6G networks will revolutionize mobile communications with improvements in reliability (from 99.999% in 5G to 99.99999%), capacity (from 10 Gbps in 5G to 1 Tbps), and extremely massive connectivity. These advancements are driven by novel transmission technologies,

enhanced security, and AI integration [2]. Meticulous planning and a complete overhaul of 5G networks are vital to meet 6G's requirements. Performance analysis is necessary to evaluate 5G and B5G configurations for expected performance.

A thorough review of 5G standards identifies components that may impair network performance (e.g., channel model, estimation, synchronization). An essential aspect of NR is the development of channel models, which have received considerable attention and impact from the research community [3,4]. The primary models of the 3rd Generation Partnership Project (3GPP) standard are Clustered Delay Line (CDL) and Tapped Delay Line (TDL) with variations for Line of Sight (LoS) and Non-Line of Sight (NLoS) scenarios [5]. These models

E-mail addresses: juan.belesaca@ucuenca.edu.ec (J.D. Belesaca), andres.vazquezr@ucuenca.edu.ec (A. Vazquez-Rodas), luis.urquiza@epn.edu.ec (L.F. Urquiza-Aguiar), jose.vega.sanchez@udla.edu.ec (J.D. Vega-Sánchez).

https://doi.org/10.1016/j.adhoc.2024.103609

Received 30 May 2024; Received in revised form 15 July 2024; Accepted 22 July 2024 Available online 26 July 2024

^{*} Corresponding author.

play a crucial role in wireless mobile networks, especially in the new 5G radio (5G-NR), impacting areas such as channel estimation and simulation outcomes [6]. It is worth highlighting that the CDL and TDL channel models have been broadly tested and validated through real-world measurement campaigns at different frequency operations (e.g., at millimeter wave for 5G and beyond networks). In this context, in [7], the authors proposed an enhanced version of the CDL model, namely, a geometry-based clustering approach to accurately characterize the total number of clusters of scatterers produced by surrounding walls or objects obtained from outdoor measurements at 28-30 GHz for both LoS and NLoS scenarios. Herein, the results showed that the proposed approach based on the CDL premises is more physically interpretable despite the complex propagation environment. On the other hand, the empirical COST 207, ITU-R, or WINNER II models, which are based on extensive measurement campaigns, help to refine the TDL model to match real-world observations better. So, this validation procedure guarantees that TDL models accurately describe the multipath propagation of wireless channels. In this regard, in [8], measurement campaigns at 3-4 and 38-40 GHz for industrial internetof-things were introduced, where the WINNER II (which is linked to the TDL model) accurately fits the channel characteristic parameters, including path loss and delay spread. Likewise, CDL and TDL, together with other channel models belonging to the 3GPP standard (e.g., Knife Edge Diffraction, ASTER, and Dominant Path model), are being used by cellular operators for network planning for different 5G-NR urban macro environments, as described in [9,10].

The channel estimation method is a key aspect of practical wireless communication systems. Typically, channel estimation relies on pilot signals or reference signals such as Channel State Information Reference Signal (CSI-RS) and Demodulation Reference Signal (DM-RS) signals [11]. The 3GPP standard provides 5G channel estimation guidelines mainly based on the configuration of CSI-RS and DM-RS signals, which significantly impact CDL and TDL models [12]. Alternative techniques like the least squares estimator (LS) and CSI-RS-based schemes have been explored to enhance precision and efficiency beyond standard specifications [13]. Thus, studying the channel model, the accuracy of channel estimation, and UE-BS synchronization is crucial in the research community.

5G technology is being explored for its potential to achieve high efficiency in modern networks. In [14], the authors investigated Multiple-Input Multiple-Output (MIMO) hardware using a CDL channel emulator for NLoS scenarios based on 3GPP 5G specifications. They used a test bench and an anechoic chamber to determine the optimal wavelength for 5G network compatibility. In [15], researchers assessed the performance of a 5G MIMO system with frequency domain precoding in a TDL channel model under LoS conditions. The study suggests that spatial correlation in realistic systems can have a positive effect at high Delay Spread (DS) values, enhancing future network performance and reliability. Likewise, channel models have been extensively studied. [16] develops a TDL model for railway and high-speed train environments, establishing power, delay, and Doppler spectrum parameters. [17] examines CDL channel models, focusing on delay spread and angle of arrival in rural areas for MIMO with SP and DP antennas. [18] enhances CDL model precision and validates improvements with mm-Wave band measurements.

Regarding channel estimation, the authors of [19] showed that an efficient management of the pilot signal system can significantly reduce energy consumption. An alternative channel estimation method is presented in [20], where the estimation is enhanced using two-phase intelligent reflective surfaces (IRS). In Phase 1, the reflection phase shifts of IRS 1 are fixed, while the phase shifts of IRS 2 are dynamically adjusted to facilitate the end-to-end channel estimation. In Phase 2, both the double and single reflection channels are efficiently estimated by exploiting the intrinsic relationship between them, thereby reducing signal overload and achieving high estimation precision. Similarly, under the same channel estimation principle for IRS, [21] employs a

design based on a Minimum Variance Unbiased Estimator to reduce computational complexity and improve estimation accuracy.

With respect to synchronization, the method in [22] simplified SSB beamforming and additional data/control transmission initiation. Precise time–frequency synchronization is critical for PDSCH decoding; errors can impair system performance and require multiple SSB measurements, potentially increasing energy consumption. To address these challenges, [23] proposed an improved paging monitoring approach to reduce interruptions in idle mode reception. Precise time–frequency synchronization is vital for reliable PDSCH decoding and requires optimization through multiple SSB measurements.

Artificial Intelligence (AI) is revolutionizing various domains by enhancing problem-solving and data processing. In communication systems, AI-driven techniques improve performance, efficiency, and reliability. Deep learning algorithms enable new methods for channel estimation, offering more accurate communication in challenging environments. In 5G networks, [24] introduced a deep learning algorithm for channel estimation using a 2D image to represent the time–frequency channel response. The authors utilized deep convolutional neural networks (CNN) for high-resolution image recovery, employing super-resolution and image restoration to estimate channel responses from DM-RS signals. Their algorithm outperformed classical channel estimation techniques.

Likewise, the authors in [25] employ deep neural networks (DNN) for channel estimation within massive MIMO systems, leveraging deep image prior (DIP) for denoising and least-squares (LS) estimation. The DNN architecture adapts to 3D communication signals, reducing pilot signals by learning from interference-free ones. Neural networks for channel estimation require careful training consideration due to their sensitivity [26]. Similarly, [27] proposes a method where the neural network assigns pilot signals non-uniformly across subcarriers, reducing overload and enhancing channel estimation via pilot signal diversity.

Conversely, the advancement of 5G testing software is crucial for detailed analysis of 5G network performance, enabling simulations that closely replicate real-world scenarios without the high costs of full-scale network deployments. Well-known computational tools like OpenAirInterface (OAI) and Matlab are well-known for their ability to support various network configurations in evaluating 5G network performance. The OAI platform includes the Demodulation Reference Signal (DM-RS) configuration in the PDSCH. On the other hand, Matlab's 5G toolbox allows the use of essential 5G network parameters such as demodulation algorithms [28], coding techniques [29], channel estimation methods [13], and synchronization algorithms [22], among others. These software tools offer essential resources for comprehensive and cost-effective performance assessments.

Despite extensive 5G research, the combined effects of (i) signal strength, (ii) channel estimation in CDL and TDL models, and (iii) synchronization on 5G performance have not been fully explored. The key takeaways of this paper are the following:

- We analyze 5G networks under 3GPP models, focusing on channel estimation and synchronization.
- We compare MIMO channel estimation performance using CNN and traditional methods.
- We extend our analysis to channel estimation for B5G networks, highlighting future mobile technologies.

We chose the MATLAB 5G Toolbox for this research because it provides an extensive simulation environment for 5G systems, enables the quick design and validation of algorithms, ensures the adherence to 3GPP standards and offers advanced channel modeling capabilities. These attributes guarantee that our simulation results are reliable and applicable for both current and future applications.

The paper is organized as follows: Section 2 covers the theoretical background of 5G and 5G advanced architecture, including physical

layer components, signals for channel estimation and synchronization, channel models, and a brief on convolutional neural networks. Section 3 details the methodology and scenarios for simulation tests. Section 4 discusses simulation results and insights for maximizing 5G benefits. Finally, Section 5 presents conclusions and future research directions.

2. Theoretical background

The 5G architecture based on 3GPP standards (release 17) is briefly introduced in this section. Furthermore, the physical layer is described in terms of channels and signals. Finally, the CDL and TDL channel models are reviewed.

2.1. General aspects of 5G

5G technology represents a major advancement in mobile networks, offering high data rates and numerous new services. It supports applications like Device-to-Device (D2D) communication, Massive Machine-Type Communications (M-MTC), enhanced Mobile Broadband (eMBB), Ultra-Reliable Low Latency Communication (URLLC), and Vehicle-to-Everything (V2X) connectivity. These services necessitate exploring new frequency bands, including millimeter waves, to meet growing bandwidth demands and enable high-speed networks [30].

In the rapidly changing telecommunications field, the need for highly efficient networks is paramount. As the number of connected devices rises and data usage increases, it is important to ensure communication systems meet these demands in a sustainable and resource-efficient manner. Hence, evaluating 5G and investigating efficient strategies is vital. By analyzing 5G performance indicators and pin-pointing areas for optimization, we can create more effective communication protocols, access techniques, and network structures. This efficiency not only enhances connectivity and reliability for users but also opens up possibilities for future technologies and applications [31].

2.2. 5G network architecture

The 5G network architecture is not just about fast and reliable connectivity; it enables diverse services and applications across the Internet. This includes new concepts in C-IoT, Vehicle-to-Everything, and Machine-to-Machine. Both 5G and 5G Advance use the New Radio (NR) interface, supporting all these services [30,32].

The 5G network architecture supports fast and reliable connectivity for various Internet applications and services. It comprises the core 5G network (5GC) and the 5G access network. The core network is segmented into network functions (NF) for task decentralization. The access network, known as the next-generation radio access network (NG-RAN), connects NR and LTE devices through control and user plane protocols [30]. 5G infrastructure includes the RAN, core network, backhaul, and transport networks. RAN dominates the 5G infrastructure market, with virtual and centralized RAN (C-RAN) deployments increasing operational efficiency [33]. The 5G architecture uses C-RAN for ultra-fast Internet connectivity, with the 5GC being completely software-based and cloud-native, providing secure connectivity and access to various services for end users [34].

Fig. 1 shows a general description of the architecture of the 5GC and NR-RAN systems. The 5GC system is represented by interfaces based on services and reference points, which allow modeling interactions between architectural entities. The main NFs are described below.

 The Access and Mobility Function (AMF) manages the control plane interface with NG-RAN and UEs, connections, registrations, mobility, transporting messages between UEs, and the session management function (SMF), authorize and authenticate access, among others. In addition, it has the non-access stratum (NAS) security and signaling feature and mobility management in the idle state with paging control [5,30].

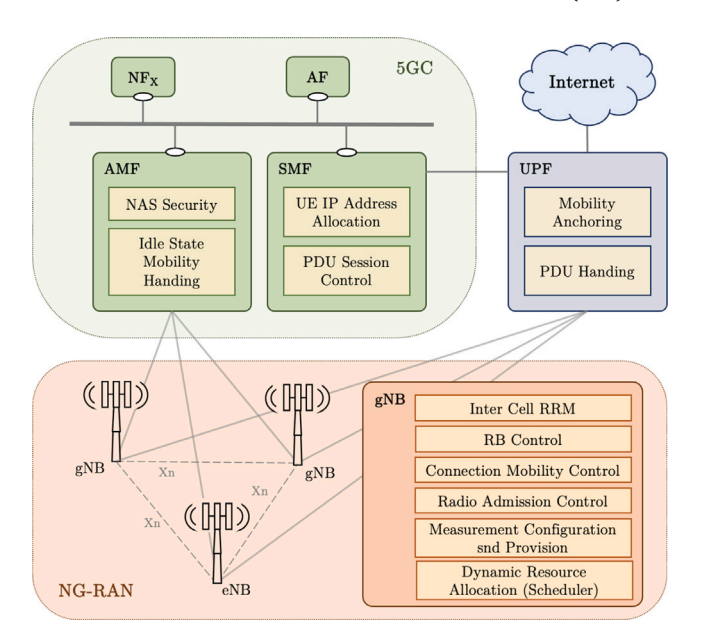


Fig. 1. Overview of the 5G system architecture and access network.

- The Session Management Function (SMF) is the entity in charge of the management of the session of the user plane, manages the IP addresses of the UEs, and manages the selection and control of the Protocol Data Unit (PDU) to route traffic to the correct destinations, among others [30].
- The Application Function (AF) manages applications and provides core network services.

Concerning to NR, it introduces a new User Plane Function (UPF) that works as an anchor point for internal or external mobility to the data network. In addition, this entity is responsible for packet routing and forwarding, packet inspection, and everything related to data traffic [30,35]. In the same way, NG-RAN allows access to the nodes of the gNB base station belonging to NR and the nodes of the Evolved Node B (eNB) belonging to the LTE BS. The Next Generation Node B (gNB) and the eNB are two integral components of the 5G architecture, which are interconnected through the Xn interface. Additionally, both are linked to the 5GC, enhancing the network's capabilities. The gNB, an essential 5G component, provides NR user plane and control plane protocol terminations towards the UE and manages radio resource management: radio bearer control, radio admission control, connection mobility control, dynamic allocation of resources, etc. [5,30]. Communication protocols between UE, gNB, and 5GC are distributed across control and user planes. This study explores the role of the physical layer within this complex network architecture.

2.3. 5G NR network physical layer

The physical layer plays a key role in the 5G NR network by handling baseband modulation of signals on the radio interface, encoding/interleaving, decoding, and mapping for multiple antennas. It selects the appropriate modulation and coding scheme, as well as the multiantenna transmission mode (i.e., MIMO setup), to ensure the desired reliability, robustness, and performance in mobile NR communications [30,31]. In addition, it provides services to the MAC medium access control sublayer and processes MAC PDUs [30]. A critical aspect of the physical layer is the downlink (DL), which comprises functional blocks and protocols configured based on various information gleaned from the physical DL channel, such as the use case and implementation scenario [30]. The subsequent section describes the channels and signals within the physical layer.

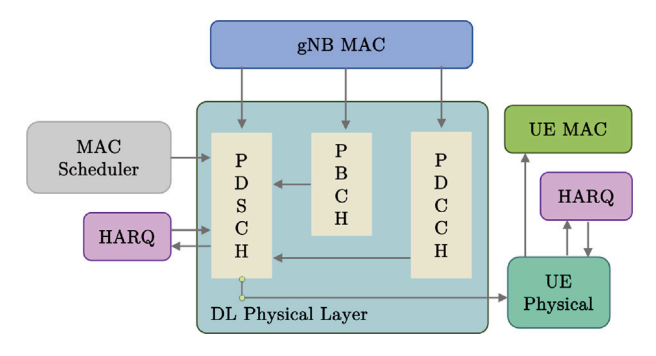


Fig. 2. Overall downlink physical layer interaction.

2.4. DL physical layer channels and signals

The DL physical layer processes the information received from the gNB MAC, UE MAC, and MAC scheduler and manages the hybrid automatic repeat request (HARQ) process. This layer segments the information into three distinct channels: the Physical Downlink Shared Channel (PDSCH), the Physical Downlink Control Channel (PDCCH), and the Physical Broadcast Channel (PBSCH). The PBCH is responsible for transmitting essential information (such as system bandwidth and system frame number within the Master Information Block (MIB)) from the base station to all UEs in a cell, enabling them to understand the network configuration and begin communication. The PDCCH helps UEs identify their allocated resources (scheduling), process data by providing HARQ information, and adjust power levels, thereby playing a crucial role in the network's coordination and efficiency. This study concentrates on the PDSCH, the main data channel that delivers user data from the base station to the UE, with its performance determining the quality and reliability of the data services provided to users [30,31].

The 5G MAC layer, defined in 3GPP Technical Specification 38.321, manages radio resources and ensures efficient communication in 5G networks. Positioned above the physical layer and below the radio link control and packet data convergence protocol, it controls access to shared radio resources, schedules transmissions, and manages services and functions [36].

Fig. 2 illustrates the DL physical layer channels and their interaction with the HARQ and Medium Access Control (MAC) processes.

2.4.1. PDSCH downlink channel

The Physical Downlink Shared Channel (PDSCH) is essential for unicast data transmission in 5G networks [31]. It accommodates modulation formats like QPSK, 16QAM, 64QAM, and 256QAM, as well as Low-Density Parity Check (LDPC) channel coding [5]. Additionally, the number of antennas determines the transmission flows. Specifically, these flows are structured based on transmission layers and codewords, which are produced at the transport channel's output and serve as the input data for the physical layer. The PDSCH supports a maximum of two codewords [30]. Depending on the precoding scheme employed, the PDSCH can transmit one or two coded transport blocks simultaneously. The processing chain of the PDSCH encompasses several critical steps that are detailed in Fig. 3 and described below:

- Transport Block CRC Attachment: A cyclic redundancy check (CRC) is employed to identify errors in transport blocks. The CRC parity bits are computed using the complete transport block.
- Code Block Segmentation and CRC Attachment: The block of bits is divided into smaller segments with a 24-bit CRC added to each segment. Then, the data is processed through LDPC encoding for error correction.
- Channel Coding: The code blocks are subjected to turbo coding to enhance error correction and increase channel capacity.

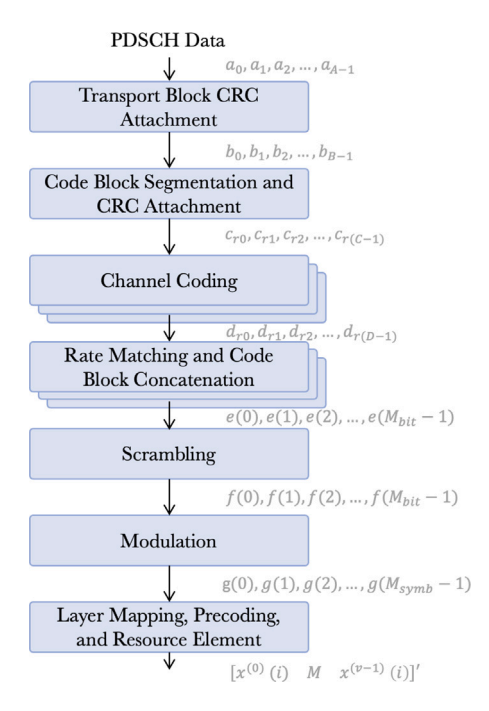


Fig. 3. Simplified functional diagram of the PDSCH processing chain.

- Rate Matching and Code Block Concatenation: Turbo-coded blocks undergo rate matching and concatenation to form the output of the channel coding process.
- PDSCH Scrambling: Codewords are scrambled using orthogonal and user equipment-specific sequences to generate sequences before modulation.
- Modulation: Scrambled codewords are subjected to QPSK, 16-QAM, 64-QAM, or 256-QAM modulation depending on the conditions of the channel.
- Layer Mapping, Precoding, and Resource Element Mapping: Following modulation, codewords are subject to layer mapping, precoding, and resource element mapping before being transmitted.

Finally, PDSCH processing ensures efficient and reliable data transmission by following these detailed steps in the downlink shared channel chain.

2.4.2. Reference signals

Within the DL physical layer, reference signals or pilot subcarriers are used to facilitate the estimation of the multipath communication channel and the reliable detection of control/traffic channels. The main reference signals are summarized in Table 1.

2.4.3. Channel estimation

Channel estimation in the PDSCH relies on reference signals such as CSI-RS and DM-RS. These signals facilitate the estimation of the channel as well as the subsequent selection of suitable precoding matrices for beamforming. The channel estimation process involves inserting known DM-RS pilot symbols into the transmission, enabling the interpolation of the remaining channel response between the transmitter and receiver. This process initiates when the UE receives the CSI-RS signals. Conversely, the gNB receives a Precoding Matrix Indicator (PMI) to determine the appropriate Precoding Matrix (PM) for data transmission and specification. Following this, the DM-RS signals use the estimated channel matrix along with the PM to enable a secondary precoding selection procedure without a codebook, which is then transmitted to the UE. In channels using the same beam, orthogonal coefficients are assigned to each data channel via DM-RS to reduce interference [12].

Table 1
Overall reference signal.

D. 6		5 11	
Reference signal	Acronym	Description	
Demodulation reference signals	DM-RS	Mainly used for channel estimation. There is a trade-off between the accuracy of channel estimation and the density of DM-RS in time (Type A and B) and frequency (Type 1 and 2). Therefore, a DM-RS mapping with adequate density is required to maximize throughput [30,31].	
Phase tracking reference signals	PT-RS	It is used for time and frequency tracking and estimating the delay spread and Doppler spread on the UE side. In addition, it compensates for the oscillator's phase noise [30,31].	
Channel-state information reference signal	CSI-RS	Used for estimation of channel status information. In addition, it is used in beam management, time/frequency tracking for demodulation, and uplink reciprocity-based precoding, among others, [30,37].	
Tracking reference signal	TRS	TRS is a special configuration of CSI-RS. It is used for accurate time and frequency tracking and estimation of path delay spread and Doppler spread [30,38].	

Channel estimation aims to obtain channel conditions like attenuation, delay, and distortion, enabling efficient signal decoding and enhancing wireless communication performance.

2.4.4. Synchronization

During the connection procedure of a UE to the network, the UE must synchronize time and frequency with a specific gNB using synchronization signals or related SSBs and DM-RS to estimate the time offset on the physical DL channel on PBCH. BSs are structured by the primary synchronization signal (PSS) and the secondary synchronization signal (SSS). SSB impacts PDSCH decoding, so multiple SSB measurements are needed [23]. PSS and SSS help UEs enter the system, identify the radio carrier boundary and cell ID, and find reference signals for coherent demodulation of other channels [30,31].

2.5. Channel models

Channel models are critical stochastic elements in wireless mobile networks. According to [39], 5G channel models include CDL and TDL. These models simulate features such as fading channels with various delay profiles and provide information on large-scale calibration, path loss configurations, and channel impulse responses [40,41]. The 5G network architecture uses these models to improve performance and efficiency, supporting advancements like network slicing, network function virtualization, and edge computing.

2.5.1. Clustered Delay Line (CDL)

In the CDL model, the signal consists of groups with different delays. Within a group, multipath components share the same delay but have different departure (AoD) and arrival (AoA) angles [42]. A cluster represents a scattering region, and [39] specifies multiple clusters, each with specific trajectories and sub-paths. Fig. 4 shows two groups, where θ_i are the departure angles relative to the line of sight. The CDL model, used in 5G mmWave communications and implemented in Matlab's 5G toolbox, simulates link-level block error rate (BLER) and fading channels with various delay profiles [43].

2.5.2. Tapped Delay Line (TDL)

In TDL models, taps with different delays are modeled as random variables with power, delay, and Doppler spectrum information. Tap values follow Rayleigh distributions for NLoS components and Rician distributions for LoS components [44]. TDL models are suitable for indoor environments with high shadowing and penetration losses because they capture the characteristics of multipath components. Conversely, the CDL model is better for outdoor environments to model clustered delays prevalent in such scenarios [3]. According to [45], CDL and TDL have different settings for LoS and NLoS, as detailed in Table 2.

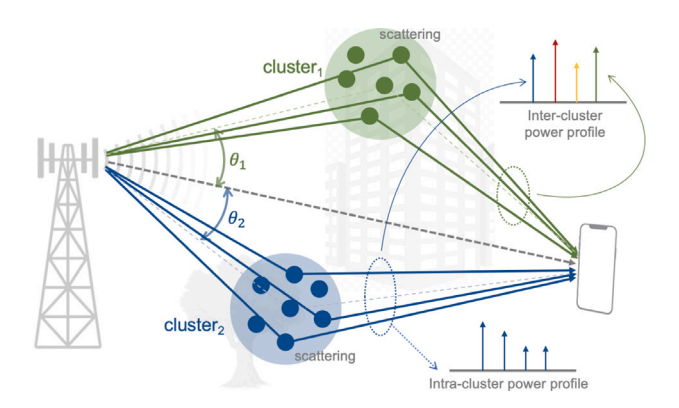


Fig. 4. Example of a CDL channel with two multipath groups.

2.6. Convolutional neural networks (CNN)

Neural networks are versatile, providing solutions in various scientific fields. Specifically, in mobile networks, they have gained significant interest in channel estimation [24,46,47]. An application in [24,48] demonstrates channel reconstruction using a CNN, similar to image reconstruction.

CNNs are deep learning models effective in processing and analyzing grid-structured data like images [49]. They use convolutional layers to apply filters and extract high-level features [50]. Inspired by the biological visual cortex, CNNs automatically learn relevant features [51]. The fundamental operation, convolution, applies filters to input data to extract specific features such as edges, textures, or colors [52].

CNNs use pooling layers, like max pooling, to reduce data dimensionality and prevent overfitting [49,50]. Regularization techniques like batch normalization and dropout further enhance model robustness and prevent overfitting [50]. Integrating various elements improves CNN efficacy in tasks such as structured grid data analysis and wireless channel state reconstruction from pilot symbols. This work uses a CNN with DM-RS pilot symbols for channel estimation, as detailed in [24], and adapts the algorithm for MIMO. The CNN-based channel estimation is compared with default interpolation-based estimation.

3. Methodology

This work identifies critical physical layer components impacting 5G NR network performance via Matlab simulations under 3GPP standards. We establish configurations for synchronization, channel estimation techniques, and network conditions for macro-urban and indoor environments using TDL and CDL models. Through ceiling analysis based on 3GPP specifications [53], we quantify the maximum theoretical performance values achievable under ideal conditions and the level of performance degradation caused by each component under

Table 2
CDL and TDL specifications.

Variation	Figure	Clusters/Taps	Power [dB]	Description	
CDL model designed for outdoor or urban environment					
A	NLoS	23	[-29.7, 0]	Selective fading with rapid changes.	
В	NLoS	23	[-14.9, 0]	Less selective fading, smoother changes.	
C	NLoS	24	[-22.8, 0]	Even less selective fading, smoother.	
D	LoS	13	[-12.5, -0.2]	Long-term shadowing, slow variations.	
E	LoS	14	[-20.6, -0.3]	Minimal shadowing for LoS.	
TDL model designed for indoor environment					
A	NLoS	23	[-29.7, 0]	Rapid time-varying fading, dense taps.	
В	NLoS	23	[-12.2, 0]	Less rapid fading, fewer taps.	
С	NLoS	24	[-22.8, 0]	Moderate fading with clustered taps.	
D	LoS	13	[-30, -0.2]	Slow-varying fading, isolated taps.	
E	LoS	14	[-29.8, -0.3]	Minimal time variations, LOS conditions.	

realistic/practical operating conditions. Finally, we compare findings with a convolutional neural network-based channel estimation method.

We describe the ceiling analysis procedure, including configuration parameters, simulation environments for evaluating PDSCH in 5G NR, and CNN channel estimation method. We define performance evaluation criteria and evaluate channel estimation using potential numerology for 5G Advance or 6G based on 3GPP release 17 [54] to assess maximum achievable performance under high-performance system configuration.

3.1. Ceiling analysis

We first analyze the PDSCH under TDL and CDL models using the Matlab 5G NR toolbox [43]. The evaluation includes perfect and practical conditions, with a focus on synchronization and channel estimation. Channel estimation uses CSI-RS and DM-RS, while synchronization uses PSS and SSS. We then use the 3GPP recommended 5G network configuration [45,53], followed by simulations with the highest capacity configuration per 3GPP release 17 [54]. This aims to meet performance benchmarks for next-generation networks, aligned with the upcoming B5G standard.

In addition, in the simulations, perfect channel estimation and synchronization for each channel model is assumed. Subsequently, the performance is assessed, considering only synchronization based on reference signals. Finally, a practical scenario is established that simulates channel estimation and synchronization using reference signals. The network throughput, as a function of the signal-to-noise ratio (SNR), is comprehensively analyzed across all these cases. Our analysis spanned urban macro (UMa) and indoor environments, providing a thorough understanding of the typical 5G configuration. This decision is prompted by the distinctive coverage attributes of small cells operating in the mmWave band. In both scenarios, the simulations are conducted using the PDSCH Matlab component, which accounts for various CDL and TDL configurations under NLoS and line-of-sight (LoS) conditions.

Initially, the simulations presume ideal channel estimation and synchronization for each channel model. Next, the performance is evaluated with synchronization based on reference signals alongside perfect channel estimation. Lastly, a realistic scenario is set up that mimics channel estimation and synchronization using reference signals. Network throughput as a function of SNR is analyzed for urban macro (UMa) and indoor environments, reflecting typical 5G setups. The analysis is driven by the unique coverage of small cells in the mmWave band. Simulations use the PDSCH Matlab component for various CDL and TDL configurations under NLoS and LoS conditions.

Lastly, in exploring the possible numerology of 5G advancements, a simulation within an indoor setting is performed using a specialized TDL channel model to evaluate the expected performance metrics for the next-generation mobile networks.

Table 3
Reference signal parameter settings.

Parameters	Value
DM-RS in time	Туре А
DM-RS in frequency	Type 2
DM-RS additional position	1 symbol
PT-RS time density	2 symbols
PT-RS frequency density	2 symbols

3.2. Experimental setup for 5G NR: Configuration parameters and simulation environments

To evaluate the effects of channel estimation and synchronization under TDL and CDL channel conditions, we perform simulations using a conventional 5G NR system consisting of currently available gNB and UE. The characteristics of the reference signals used in the communication system model are defined in Table 3.

These parameters are crucial in estimating and transmitting signals within the underlying system. The detailed configuration of the physical layer is presented in Table 4. These parameter settings are consistently applied in UMa and indoor environment simulations.

An apparent distinction between 5G NR and LTE is incorporating various environments. In this study, we evaluate two environments, UMa and Indoor, to assess the system's performance under these models. These environments have been chosen because of their contrasting characteristics and diverse applications. The specific details of each environment are described below.

3.2.1. Indoor environment

This scenario aims to replicate the characteristics of indoor deployments, such as office environments and shopping malls. Office environments often include cubicle areas, closed offices, open spaces, and corridors. Shopping malls typically span 1–5 stories and may feature a central open area accessible from multiple floors. In this scenario, the gNBs are typically mounted on ceilings or walls at 2–3 m height, while the UEs are approximately 1.5 m above the ground. Please refer to Table 4 for the specific configuration details of this scenario, as outlined in [45].

3.2.2. Urban Macro environment (UMa)

The Urban Macro (UMa) scenario aims to replicate an open area resembling a densely populated city with tall buildings. The typical coverage area spans approximately 200 m, and the gNB is mounted approximately 25 m above the surrounding building roofs. The user equipment is positioned between 1.5 and 2.5 m in height. For this scenario, the specific configuration based on [45] is presented in Table 4, which describes the parameters relevant to the UMa environment.

It is essential to mention that the specific environment in the toolbox 5G NR is characterized using channel configuration parameters such as Desired Delay Spread (DSD), Sub-Carrier Frequency Spacing (SCS), Number of Resource Blocks (NRB), and Cyclic Prefix (CP).

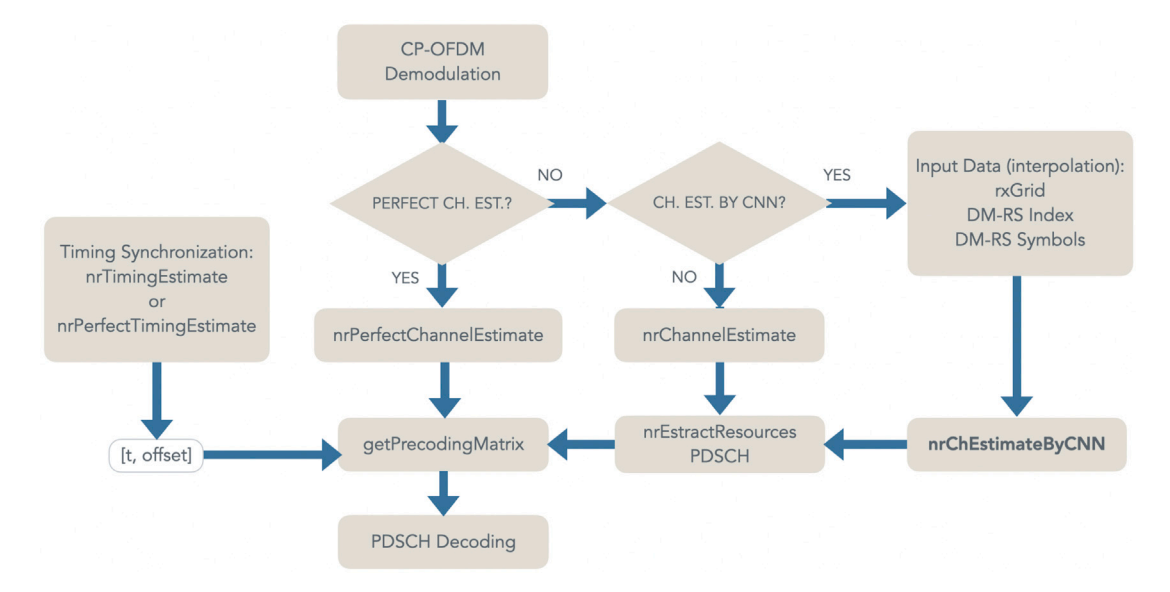


Fig. 5. Enhanced depiction of channel estimation by CNN within the downlink process flowchart for Matlab's PDSCH.

3.3. Channel estimation based on convolutional neural network

In channel estimation based on CNN, the main idea is to estimate the time–frequency channel response akin to a 2D image, utilizing DM-RS reference signals. Therefore, the CNN retrieves the channel response as a high-resolution image, as demonstrated in [24]. The architecture of the CNN is based on the Super-resolution CNN [55]. For the initial phase, an interpolation scheme approximates the channel response values through a convolutional layer employing 64 filters of size 9 \times 9, followed by ReLu activation. Subsequently, resolution enhancement is achieved using a three-layer convolutional network comprising 32 filters of size 5 \times 5, each followed by ReLu activations. The final layer employs a single-size filter of 5 \times 5 to reconstruct the image. Also, the CNN is trained using a dataset of reference signals with their respective channel responses. This study utilized a dataset of 16,000 samples, partitioned into 70% for training and 30% for validation.

In this work, the channel estimation by CNN is performed in a MIMO (8 \times 2) environment for the configuration described in Table 4. Therefore, the modified implementation is depicted in Fig. 5. The application begins after the CP-OFDM Demodulation process, which obtains the DM-RS symbols for each transmission layer. Later, the type of estimation required is determined. In the case of CNN-based channel estimation, the input data consists of the Orthogonal Frequency Division Multiplexing (OFDM) grid solely with the indices and DM-RS symbols of each receiving antenna corresponding to the transmitting antenna. The input data enters the CNN and generates a channel estimation, which then undergoes the process of resource extraction and precoding matrix determination.

3.4. Experimental numerology for B5G: Configuration parameters and simulation environments

As a final contribution of this study, we analyze the effect of channel estimation using potential numerology for B5G and 5G Advance networks to achieve maximum system performance. The configuration and numerology leverage mmWave frequency ranges with a bandwidth of 2 GHz, aiming to optimize data rates and network performance in high-capacity scenarios. This leads to limited coverage configuration for small cells, as radio waves cannot propagate over long distances due to operating frequencies. By implementing these parameters in the simulations, we focus on assessing the network's capability to handle increased data demands and exploit the advantages of mmWave technology for enhanced throughput and efficiency for future mobile

Table 4
Physical layer parameter settings for 5G NR.

Parameters	Value		
Transmission Antennas (Tx):	MIMO: 8		
Reception Antennas (Rx):	MIMO: 2		
Frequency Range (FR):	FR1: 410 MHz-7.125 GHz		
Equalizer:	Minimum Mean Square Error (MMSE)		
Beamforming:	Hybrid Analog-Digital		
Scheduling:	Hybrid ARQ (HARQ)		
Channel Encoding and Decoding:	Layered belief propagation (LDPC)		
Modulación:	16QAM		
Target Code Rate:	378		
PDSCH allocation:	All 14 symbols		
Environment:	UMa	Indoor	
Delay Spread Desired (DSD):	363 ns (normal)	30 ns (normal)	
Sub-Carrier Spacing (SCS):	30 kHz	30 kHz	
Number of Resource Blocks (NRB):	65	51	
Bandwidth (BW):	25 MHz	20 MHz	
Cyclic Prefix (CP):	2.3 µs (normal)	2.3 µs (normal)	
gNBs' Antennas height (Tx):	25 m	2-3 m	
UE's Antennas height(Rx):	1.5-2.5 m	1.5 m	

Table 5Physical layer parameters setting for B5G.

Parameters	Value	
Transmission Antennas (Tx)	MIMO: 128	
Reception Antennas (Rx)	MIMO: 4	
Frequency Range (FR)	FR2-2: 52.6-71 [GHz]	
Equalizer	Minimum Mean Square	
	Error (MMSE)	
Beamforming	Hybrid Analog-Digital	
Scheduling	Hybrid ARQ (HARQ)	
Channel Encoding and Decoding	Belief Propagation	
	(LDPC)	
Modulation	256QAM	
Target Code Rate (TCR)	4/5	
PDSCH allocation	All 14 symbols	
Small cell (Indoor)		
Channel model	TDL	
Delay Spread Desired (DSD)	50 ns (normal)	
Sub-Carrier Spacing (SCS)	960 kHz	
Number of Resource Blocks (NRB)	148	
Bandwidth (BW)	2 GHz	
Cyclic Prefix (CP)	2.3 μs (normal)	

communication systems. Hence, the physical layer configuration and the characteristics of the reference signals used in the communication system are described in Table 5.

3.5. Performance evaluation criteria

Performance evaluation in UMa and indoor scenarios involved PDSCH Matlab simulations, considering various configurations of CDL and TDL in NLoS (in variations A, B, and C) and LoS conditions (in variations D and E). In the NLoS profiles, variation A represents highly dense and complex environments, while variation B represents urban areas with lower density and less temporal dispersion. Variation C corresponds to suburban or residential areas with fewer obstructions. Regarding the LoS profiles, variation D represents suburban or residential environments with consistent fading, whereas variation E corresponds to rural areas with minimal temporal variations.

Initially, simulations assumed perfect channel estimation and synchronization for each channel model. Then, 5G performance is assessed considering realistic conditions, incorporating channel estimation and synchronization based on reference signals. Then, the behavior of the channel estimation method based on the CNN is evaluated; this method is only applied to the configuration shown in Table 4. Finally, the network throughput as a function of the SNR is considered as the main performance metric to evaluate the 5G system for all the cases.

¹ These variations will be fully detailed in the following section.

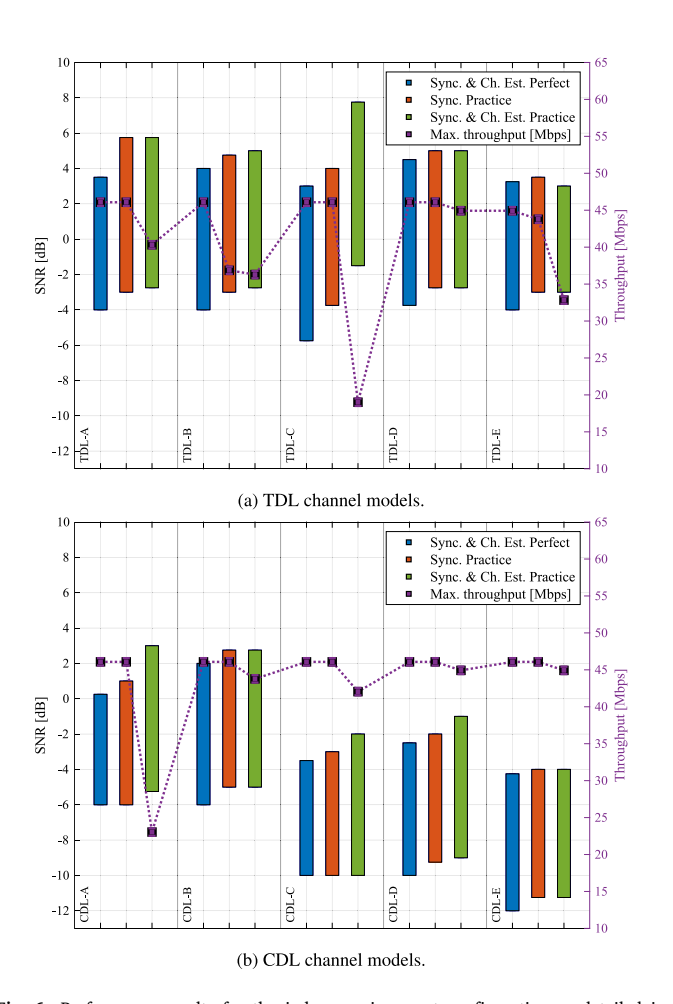


Fig. 6. Performance results for the indoor environment configuration as detailed in Table 4.

4. Simulation results and discussion

This section presents the throughput curves for 5G NR under various channel models and settings. These performance differences are shown via the throughput vs. SNR metric, spaced 0.25 dB for each model, as determined from initial testing and available computing resources. The simulations cover Indoor and UMa scenarios for each 5G NR channel model. In our configuration, Variation A signifies the environment with the highest temporal dispersion, indicating areas with dense obstacles and multiple pathways, typically used in highly urban settings and complex indoor environments such as large office buildings and shopping malls. Similarly, Variation B shows a more scattered delay profile, fitting for moderately urban regions with several reflections. Variation C illustrates settings with some obstacles and reflections, commonly observed in suburban areas. Variation D is defined by low temporal dispersion, making it suitable for residential areas with line-of-sight (LoS) conditions. Lastly, Variation E exhibits a delay profile with low temporal dispersion, ideal for rural and suburban environments with direct signal paths (LoS). Next, the simulations for numerology B5G or 5G advanced in Indoor scenarios for TDL are introduced. This comprehensive set of simulations provides a broad perspective to analyze the 5G/B5G performance across various network parameter settings. Lastly, the assessment of the 5G NR system utilizing a convolutional neural network for channel estimation is also featured.

4.1. Performance results in 5G NR

The performance curves for the indoor and UMa scenarios for 5G NR are shown in Figs. 6 and 7, respectively. Each plot in these figures

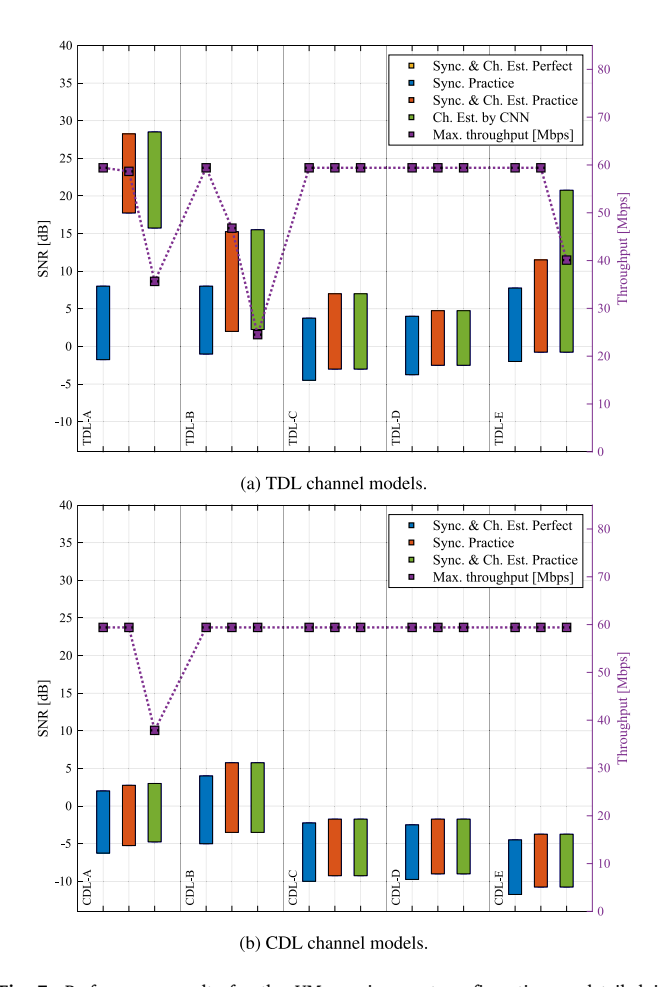


Fig. 7. Performance results for the UMa environment configuration as detailed in Table 4.

depicts the throughput and the required SNR ranges by adjusting system settings (i.e., synchronization and channel estimation) under CDL and TDL channels. The results are categorized for each channel model setup (e.g., A, B, C, D, or E) along the horizontal axis in the figures. Similarly, the right vertical axis shows the throughput values in Mbps, and the left vertical axis displays the SNR values in dB. The colors for the configurations are as follows: perfect synchronization and channel estimation (blue), practical synchronization (orange), practical synchronization and channel estimation (green). For all these cases, the SNR ranges from the lower to the upper limit, representing the minimum and the maximum SNR values at which maximum throughput is achieved. Also, the achievable throughput is illustrated on the right horizontal axis (purple).

4.1.1. Performance evaluation under indoor environments

From the illustrations in Fig. 6, it is observed that the UEs operating under TDL channels require higher received signal power than CDL environments. These results agree with what was stated in [44], where the TDL channel was explicitly designed for indoor scenarios.

Fig. 8(a) illustrates the results for NLoS variation A. From Figs. 6 and 8(a), synchronization has an average impact of 1 dB on TDL, compared to the 0.5 dB effect of channel estimation alone, and both together have a 1.5 dB effect. Notably, channel estimation has a more significant influence on CDL, with a 50% impact compared to TDL's 12.5% impact. Additionally, in the practical scenario for both TDL and CDL, there is a 2.5 dB difference, but TDL achieves higher throughput. In summary, the system under CDL channels demonstrates inferior results in this scenario primarily due to the channel estimation.

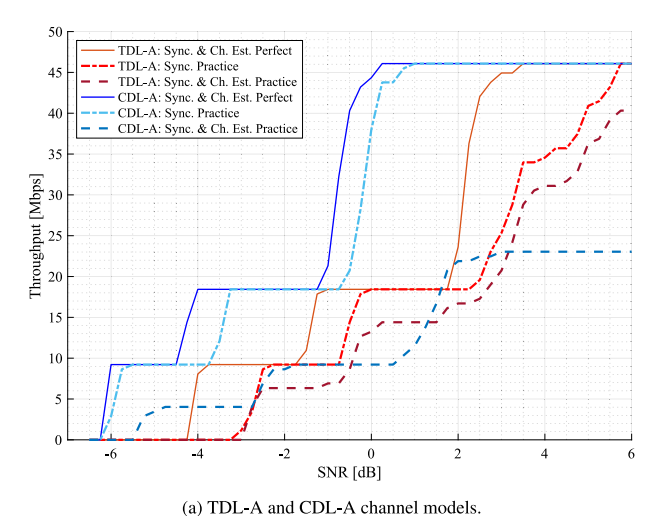
To complement the analysis, Fig. 8(b) presents the results for the variation B of NLoS. The difference between TDL and CDL is generally reduced to 2 dB for all cases. In contrast to variation A, TDL exhibits the lowest throughput with a reduction of 21.25%, and the channel estimation does not significantly impact both CDL and TDL. Consequently, both models exhibit similar behavior in this scenario. On the other hand, in variation C (Figs. 6 and 8(c)), TDL requires an average of 6.6 dB higher signal power than CDL. Interestingly, TDL achieves the lowest throughput, reaching 19.01 Mbps, primarily due to the impact of channel estimation. These results indicate that variation C represents the poorest performance for NLoS channel models in indoor environments, as it closely mimics the real-world moderate fading effects.

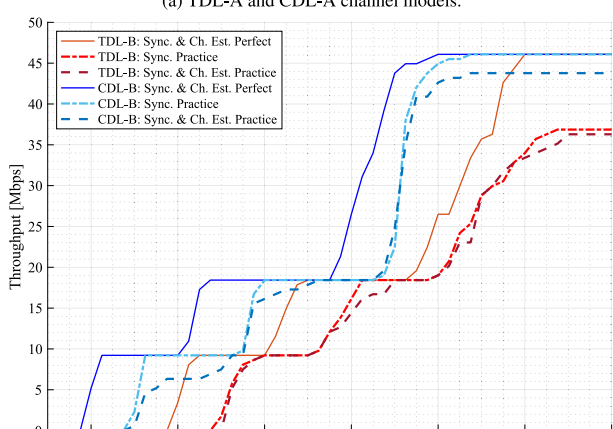
The results for the LoS channel models (variations D and E) exhibit similarities (Figs. 9(a) and 9(b)). In both cases, synchronization is the only parameter that affects the throughput, with an impact of approximately 1 dB. Moreover, TDL requires a higher received signal power, with 6.6 dB for variation D and 7.7 dB for variation E (Fig. 9). Interestingly, in the case of TDL-E, even with perfect channel estimation and synchronization, the maximum throughput is not achieved. Overall, in LoS scenarios, synchronization similarly affects both CDL and TDL.

4.1.2. Performance evaluation under UMa environments

The throughput graphs for the Urban Macro scenario are presented in Figs. 10 and 11. Similarly to the previous section, each subgraph compares the corresponding variations of the CDL and TDL models. The maximum throughput achieved and the corresponding SNR range are provided in Fig. 7. Similar to the Indoor scenario, both in NLoS and LoS cases, the system under TDL channel models requires higher received signal power than CDL.

Regarding variation A of the TDL and CDL channel models (Figs. 7 and 11(a)), the channel estimation significantly affects the maximum throughput achieved. In TDL, the maximum throughput is reduced by 40.01%, while in CDL, it experiences a reduction of 36.26%. Additionally, TDL requires approximately 15 dB higher received signal power to attain the maximum throughput.





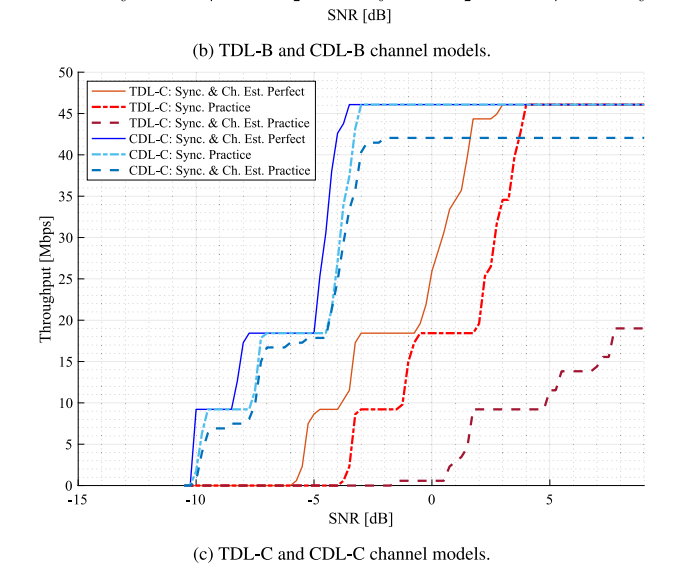


Fig. 8. Evaluation under NLoS channel models for the indoor scenario in 5G NR.

On the other hand, variation B (Figs. 7 and 11(b)) exhibits the lowest throughput in TDL, with a reduction of 58.74%. Both the channel estimation and synchronization equally influence this decrease. In the case of the system under the CDL channel, which is solely affected by synchronization, an additional 1.5 dB is required.

The results indicate that channel estimation has no significant impact on throughput in variation C (NLoS) and variations D and E (LoS). However, in the specific case of TDL-E (Fig. 10(b)), channel estimation

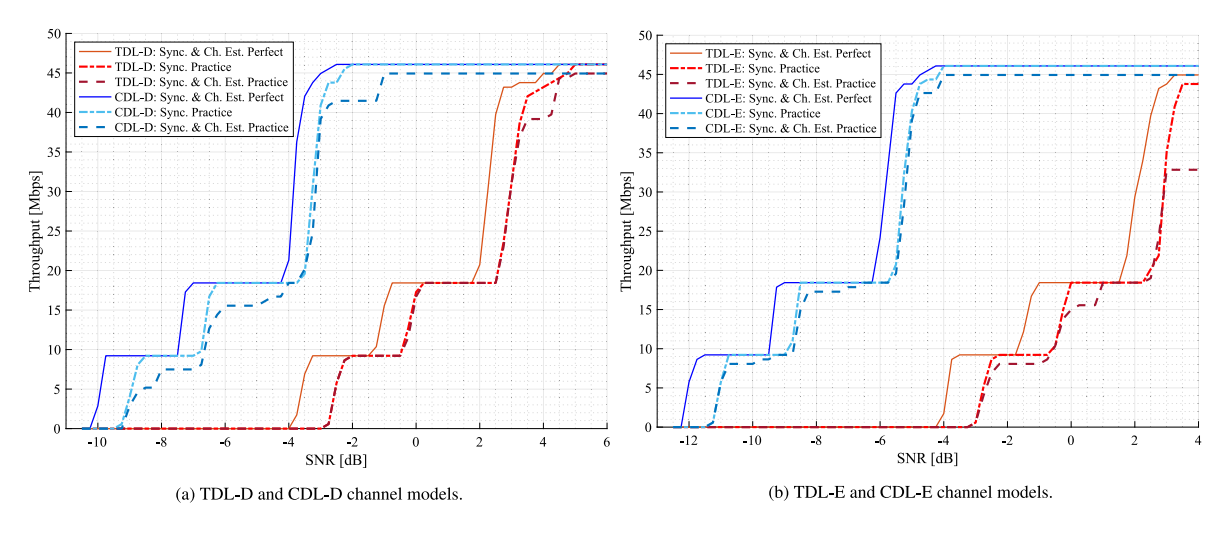


Fig. 9. Evaluation under LoS channel models for the indoor scenario in 5G NR.

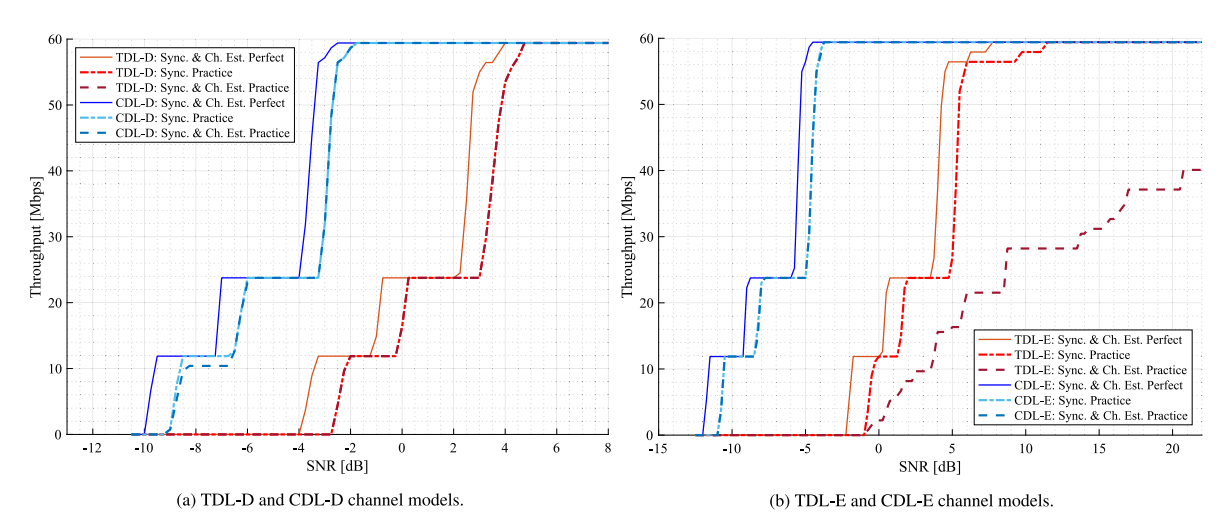


Fig. 10. Evaluation under LoS channel models for the UMa scenario in 5G NR.

reduces the maximum throughput achieved by 32.5%. In variation C, the difference between TDL and CDL is 6.9 dB, while in variation D, it is 6.4 dB. The difference widens to 10.2 dB in variation E. Notably, in both variation C (NLoS) and variation D (LoS), TDL and CDL exhibit similar behavior within the UMa scenario.

4.2. Performance results in B5G NR

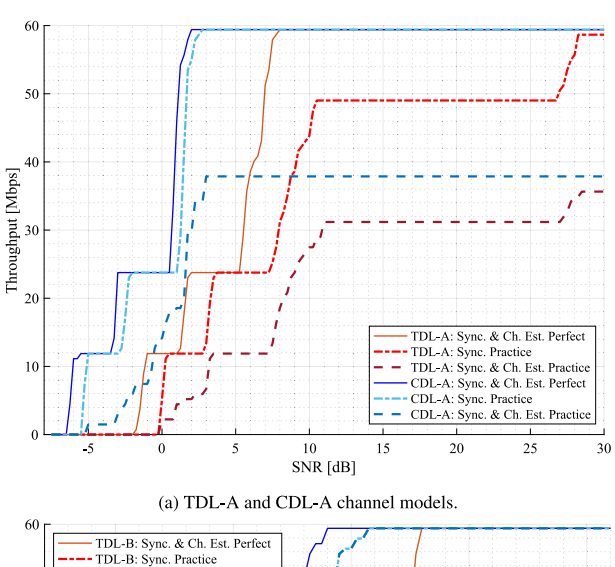
In furtherance of this study, we assess the B5G mobile system under LoS and NLoS environments of TDL channels using advanced numerology to optimize performance, as delineated in Section 2.4. Fig. 12 provides an elucidation of the performance outcomes, with TDL variants depicted in varying colors TDL-A in blue, TDL-B in orange, TDL-C in yellow, TDL-D in violet, and TDL-E in green. Each channel model is delineated by solid lines representing perfect channel estimation and dashed lines denoting practical channel estimation.

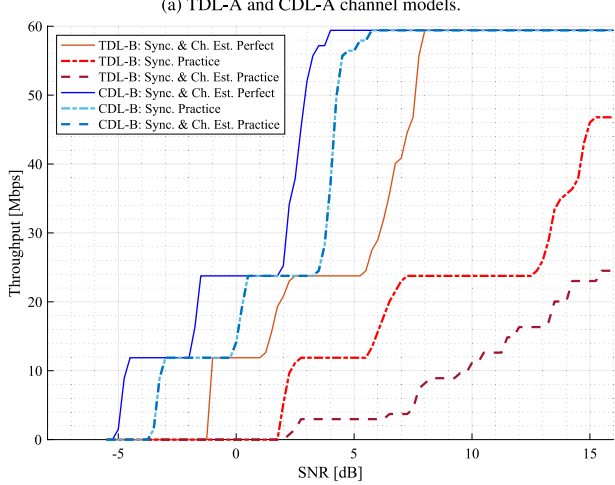
The theoretical maximum throughput achievable with the parameters delineated in Table 5 stands at 14.42 Gbps, accommodating four transmission layers (equivalent to 4 receiving antennas) by the specifications outlined in Table A.3.3.5 of [54]. Notably, variant A necessitates a higher average received signal power of 5 dB. Conversely, variant B fails to achieve the maximum throughput, reaching only 7.22 Gbps and necessitating a higher power input of approximately 6 dB. Similarly, variant C achieves a throughput of only 9.38 Gbps.

Nevertheless, the LoS environments are particularly susceptible to the impacts of practical channel estimation. Variant D experiences a significant reduction of around 35% (equating to 4.96 Gbps), demanding an SNR of 22 dB compared to the requisite 5 dB for perfect estimation. Variant E exhibits the most profound disparity, with a mere 631 Mbps throughput achieved with perfect estimation, constituting a staggering 95% reduction from the theoretical maximum throughput.

The results obtained with the anticipated numerology B5G, when compared to those for 5G in Section 4.1, demonstrate a significant increase in throughput. This improvement is primarily attributed to the increase in the number of transmission layers (from 4 reception antennas), the modulation scheme evolving from 16QAM in 5G NR to 256QAM in B5G, and the number of resource blocks increasing from 51 in 5G NR to 148. This corresponds to a 6 GHz bandwidth and 960 kHz sub-carrier spacing in B5G.

It is important to note that, as expected, achieving the throughput values shown in Fig. 12, corresponding to the numerology B5G, requires a higher SNR than those shown in Section 4.1.1 for 5G NR. Specifically, for Variation A B5G, at least 5 dB more SNR is needed compared to 5G NR. For Variations B, C, and D, approximately 8.5 dB additional SNR is required. For Variation E, a further 17 dB is necessary. This increased SNR requirement highlights the heightened demands of new technologies to manage the complexity of communication environments.





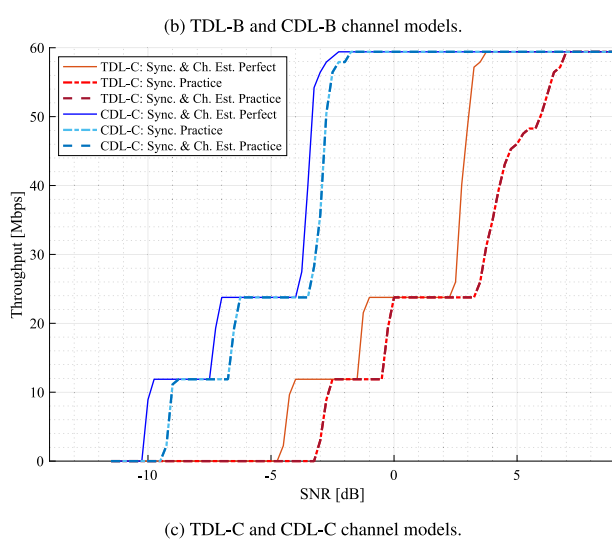


Fig. 11. Evaluation under NLoS channel models for the UMa scenario in 5G NR.

4.3. Performance evaluation of channel estimation by CNN applied to 5G NR

From the results of the previous simulations, it can be observed that the channel estimation generally has a more significant impact on the physical layer performance. Therefore, in this work, we evaluate the application of a channel estimation method based on convolutional neural networks as an alternative to improve the overall performance of

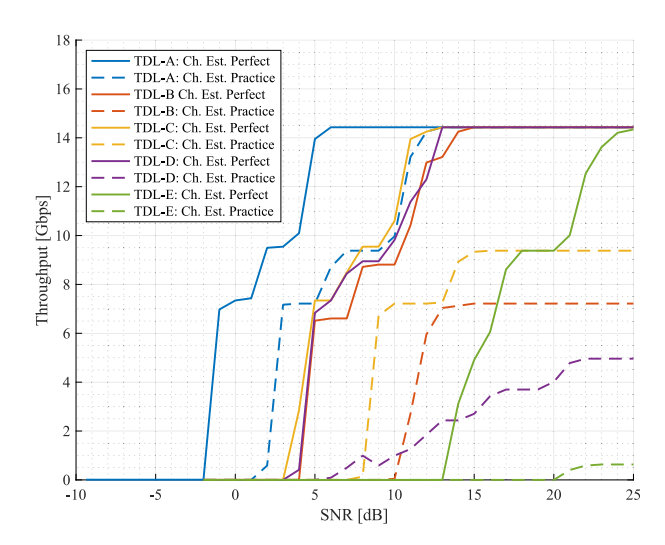


Fig. 12. Assessment of channel models for Indoor scenarios with advanced numerology B5G networks as detailed in Table 5.

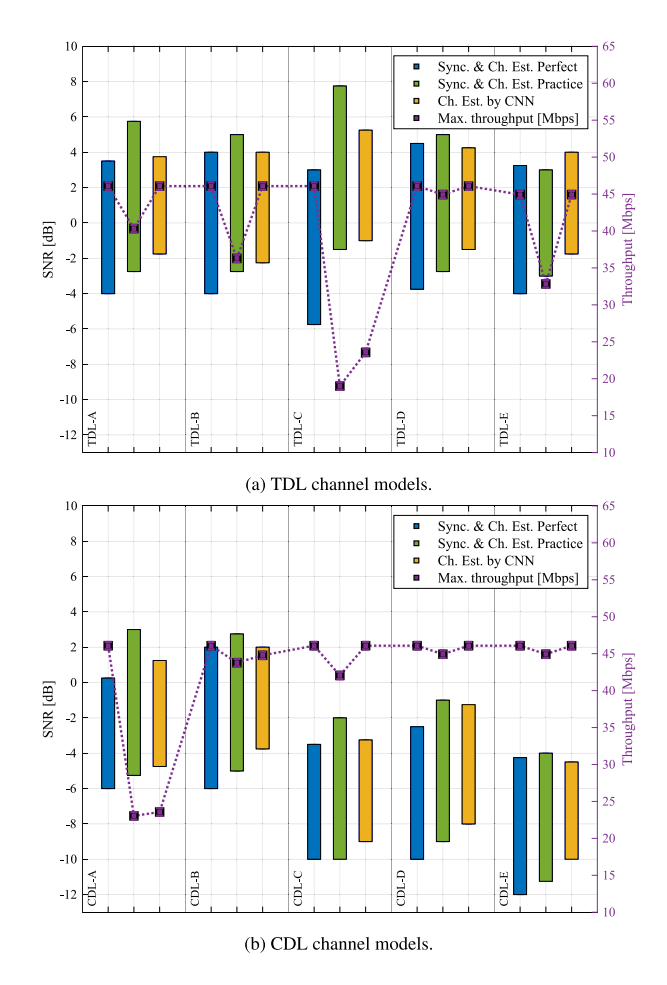


Fig. 13. Comparative performance results of channel estimation by CNN for the Indoor environment configuration as detailed in Table 4.

the mobile system. The comparative performance curves of the different channel estimation methods for indoor and UMa scenarios for 5G NR are depicted in Figs. 13 and 14, respectively. All plots in both figures show the throughput and the required SNR by varying the channel estimation method (i.e., perfect, practical, and by CNN) under CDL and TDL channels.

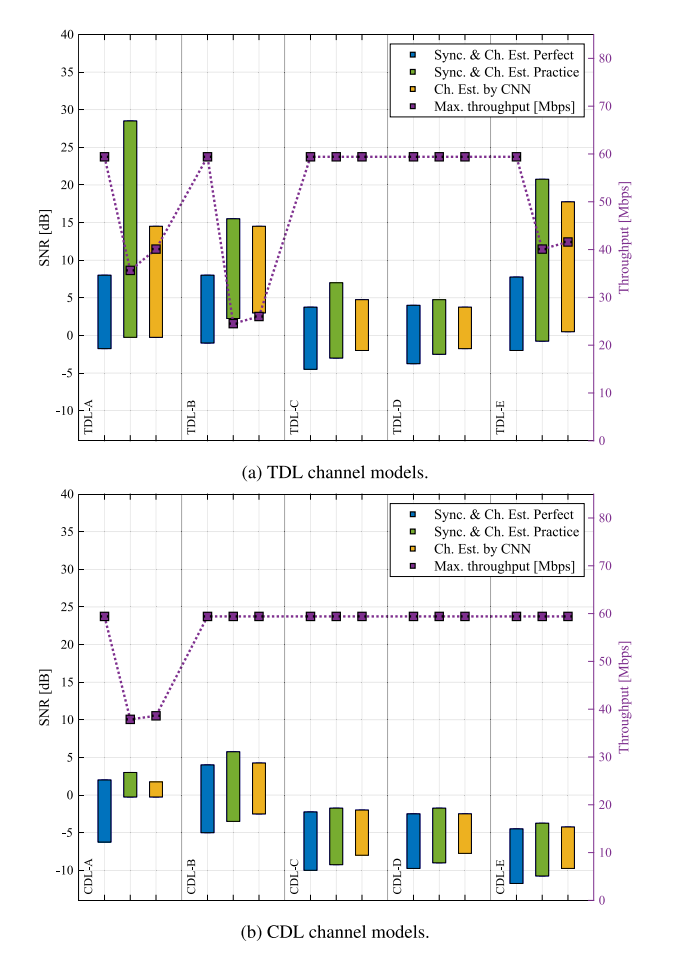


Fig. 14. Comparative performance results of channel estimation by CNN for the UMa environment configuration as detailed in Table 4.

Similar to the plots shown in Section 4.1, the obtained results are segmented for each channel model setup (e.g., A, B, C, D, or E) on the horizontal axis in the figures. Likewise, the right vertical axis displays the throughput values in Mbps, and the left vertical axis presents SNR values in dB. The colors for the system model configurations are set to: synchronization and channel estimation perfect (blue), synchronization and channel estimation practical (green), and channel estimation by CNN (orange). For all these cases, the SNR ranges from the lower to the upper limit, representing the minimum and the maximum SNR values at which maximum throughput is achieved. Also, the achievable throughput is illustrated on the right horizontal axis (purple).

For all channel models in indoor environment, the channel estimation by CNN achieves maximum throughput compared to practical channel estimation (Fig. 13). A detailed comparison is depicted in Figs. 15 and 16, which reveals that channel estimation by CNN performs less effectively at low SNR than practical channel estimation. This can be attributed to the 2D image principle employed to represent the channel response, wherein at low SNR, noise predominates in the channel response and thereby impacting performance directly. However, CNN gains an advantage with a higher SNR, outperforming the practical channel estimate in all cases and allowing maximum performance with a lower SNR (average 2.7 dB).

In the case of the UMa environment, Fig. 14 summarizes the performance results. These show that in both the TDL and CDL channel models, the channel estimation performed by the CNN shows a marginal improvement in performance, approximately 4 Mbps (TDL-A, TDL-B, TDL-C and CDL-A) compared to the indoor scenario. However, for other

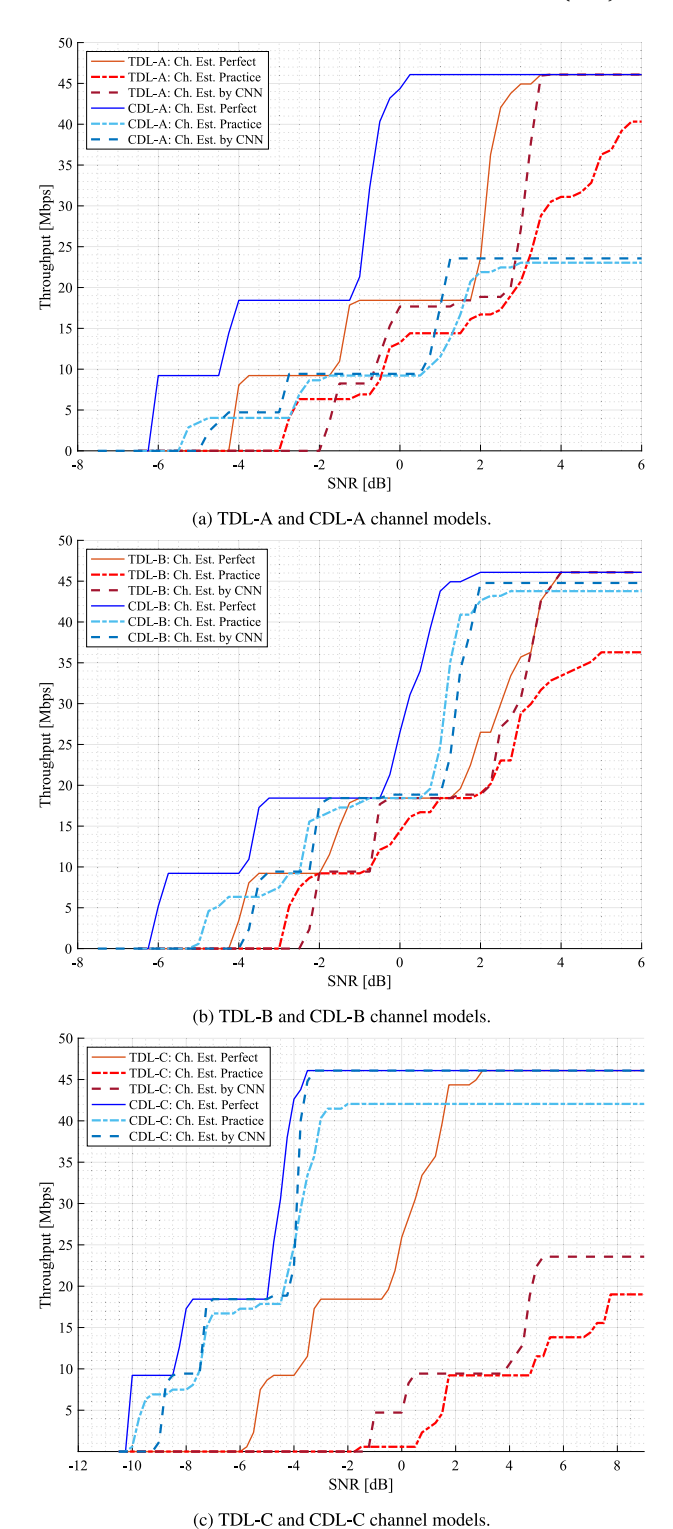


Fig. 15. Evaluation under NLoS channel models for the indoor scenario in 5G NR.

channel models, there is no significant difference in performance. It is important to note that SNR is reduced by an average of 1 dB in all cases, as seen in Figs. 17 and 18.

5. Conclusions and future works

The growth of mobile broadband and new technologies like C-IoT, D2D, URLLC, and MTC have increased demand for higher performance and lower latency. Evaluating NR system components to identify

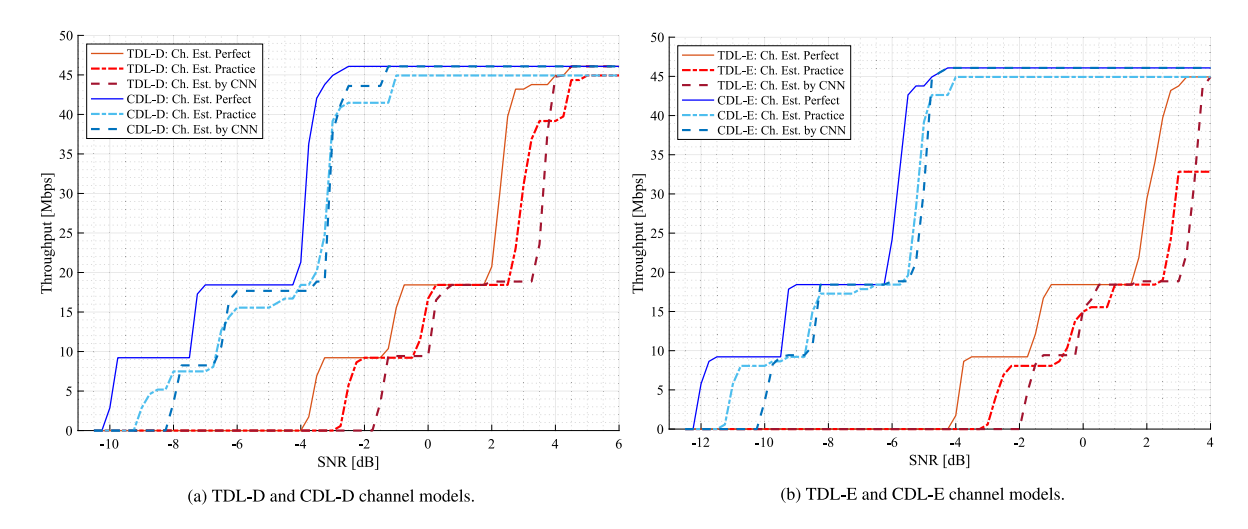


Fig. 16. Evaluation under LoS channel models for the indoor scenario in 5G NR.

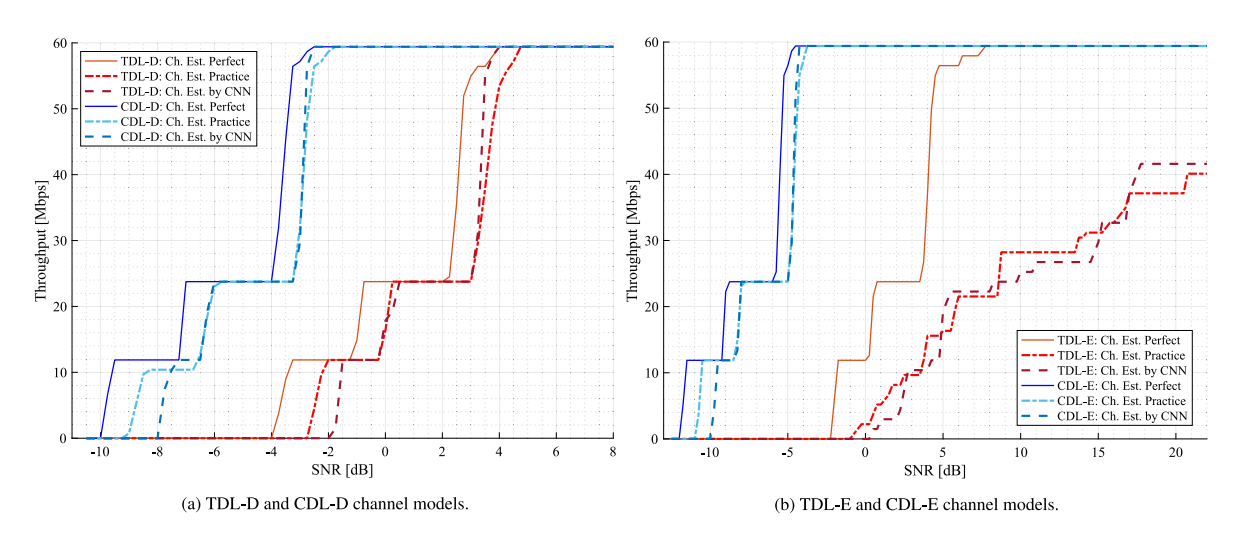


Fig. 17. Evaluation under LoS channel models for the UMa scenario in 5G NR.

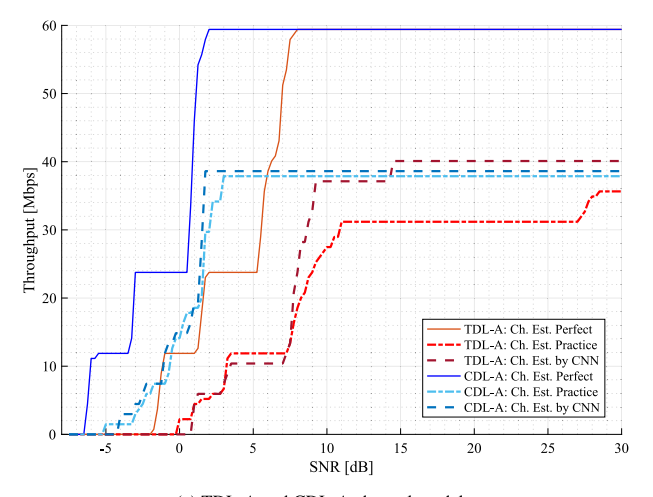
weaknesses through ceiling analysis is crucial. This can guide future research efforts to improve techniques for next-generation networks (5G Advance or 6G).

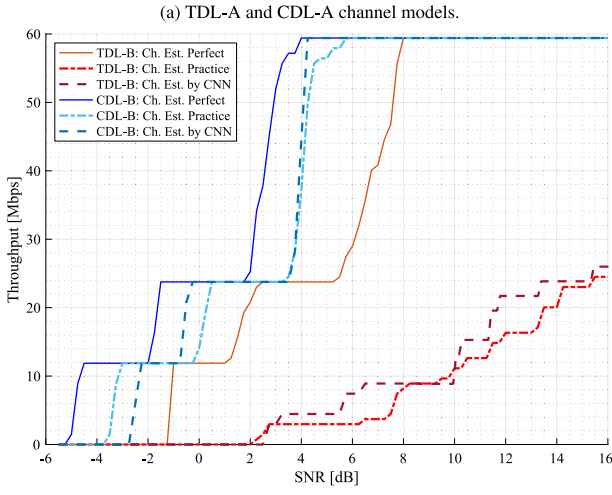
To improve CDL or TDL channel modeling techniques further, emphasis was placed on the specific environments they are intended to represent, such as Indoor or UMa. Additionally, a careful examination of the individual effects of synchronization, traditional channel estimation, and IA-based channel estimation (e.g., CNN approach) was essential. In this regard, it was noted that channel estimation and practical synchronization rely on reference signals (such as DM-RS, PT-RS, PSS, SSS) to fulfill their roles.

CNNs were trained to rebuild the channel response using DM-RS for channel estimation. On the other hand, CNN channel estimation across all TDL and CDL variations exhibited outstanding performance advantages at higher received signal powers than practical channel estimation. CNN was independently trained for Indoor and UMa scenarios, but was not applied to B5G simulations due to computational complexity.

In the case of Indoor scenarios, it was observed that channel estimation only affects the TDL-C model, while the rest of the TDL variations were significantly influenced by synchronization. Conversely, the CDL model demonstrated greater robustness, with synchronization having a relatively minor impact. Similarly, in the UMa scenario, it was seen that the system under the CDL model demonstrated robustness against channel estimation, with only minor degradation caused by synchronization. However, variation A stands out as an exception, where CDL and TDL experienced significant degradation of 40% and 36%, respectively, due to channel estimation. Contrarily, TDL exhibited proportional degradation resulting from channel estimation and synchronization in variation B.

In future research, it would be compelling to extend the ceiling analysis to encompass additional physical layer components in both downlink and uplink. This approach would allow us to further investigate and pinpoint possible enhancement areas in channel models specifically designed for the pertinent scenarios. Additionally, this study has offered valuable insights into incorporating AI as a basis for formulating strategies to improve the performance of 5G NR systems in envisaged deployment contexts.





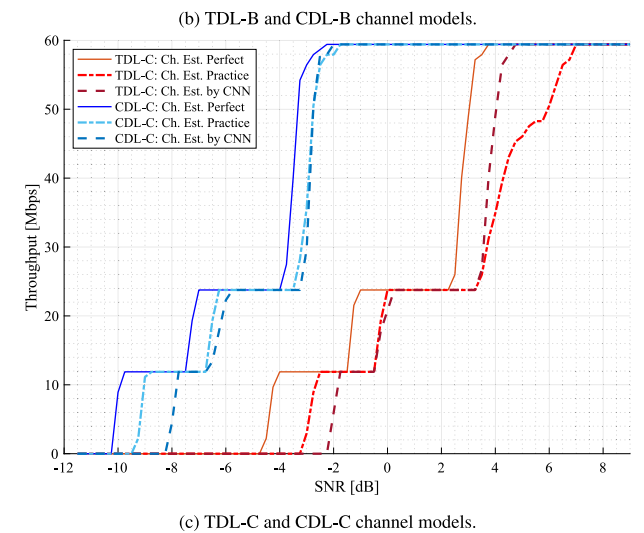


Fig. 18. Evaluation under NLoS channel models for the UMa scenario in 5G NR.

CRediT authorship contribution statement

Juan Diego Belesaca: Writing – original draft, Visualization, Software, Methodology, Investigation, Formal analysis, Data curation. Andres Vazquez-Rodas: Writing – review & editing, Writing – original draft, Validation, Supervision, Project administration, Methodology, Investigation, Funding acquisition, Formal analysis, Conceptualization. Luis F. Urquiza-Aguiar: Writing – review & editing, Validation, Methodology, Investigation, Formal analysis, Conceptualization.

J. David Vega-Sánchez: Writing – review & editing, Visualization, Validation, Methodology, Formal analysis.

Declaration of competing interest

The authors declare that they have no known competing financial interests or personal relationships that could have appeared to influence the work reported in this paper.

Data availability

Data will be made available on request.

References

- [1] Evizal Abdul Kadir, Raed Shubair, Sharul Kamal Abdul Rahim, Mohamed Himdi, Muhammad Ramlee Kamarudin, Sri Listia Rosa, B5G and 6G: Next generation wireless communications technologies, demand and challenges, in: 2021 International Congress of Advanced Technology and Engineering, ICOTEN, IEEE, ISBN: 978-1-6654-1224-7, 2021, pp. 1–6, http://dx.doi.org/10.1109/ICOTEN52080. 2021.9493470.
- [2] Ran Poliakine, What you should know about 5G technology and what the future holds, 2021, URL https://www.forbes.com.
- [3] Gordana Barb, Marius Otesteanu, On the influence of delay spread in tdl and cdl channel models for downlink 5g mimo systems, in: 2019 IEEE 10th Annual Ubiquitous Computing, Electronics & Mobile Communication Conference, UEMCON, IEEE, 2019, pp. 0958–0962.
- [4] Cheng-Xiang Wang, Ji Bian, Jian Sun, Wensheng Zhang, Minggao Zhang, A survey of 5G channel measurements and models, IEEE Commun. Surv. Tutor. 20 (4) (2018) 3142–3168.
- [5] 3rd Generation Partnership Project, 3GPP TR 21.915 version 15.0.0 Release 15, 2019.
- [6] Ayşegül İlay Tunali, Hakan Ali Çirpan, Impact of imperfect channel estimation on 5G-NR, in: 2021 IEEE International Black Sea Conference on Communications and Networking, BlackSeaCom, 2021, pp. 1–6, http://dx.doi.org/10.1109/ BlackSeaCom52164.2021.9527762.
- [7] Guojin Zhang, Jesper Ødum Nielsen, Xuesong Cai, Gert Frølund Pedersen, Wei Fan, Geometry-based clustering characteristics for outdoor measurements at 28–30 GHz, IEEE Antennas Wirel. Propag. Lett. 21 (9) (2022) 1797–1801, http://dx.doi.org/10.1109/LAWP.2022.3180179.
- [8] Yu Wang, Yejian Lv, Xuefeng Yin, Jiawei Duan, Measurement-based experimental statistical modeling of propagation channel in industrial IoT scenario, Radio Sci. 55 (9) (2020) 1–14, http://dx.doi.org/10.1029/2019RS007013.
- [9] Valdemar Ramón Farré Guijarro, José David Vega Sánchez, Martha Cecilia Paredes Paredes, Felipe Grijalva Arévalo, Diana Pamela Moya Osorio, Comparative evaluation of radio network planning for different 5G-NR channel models on urban macro environments in Quito city, IEEE Access 12 (2024) 5708–5730, http://dx.doi.org/10.1109/ACCESS.2024.3350182.
- [10] Valdemar Farré, José David Vega Sánchez, Henry Carvajal Mora, 5G NR radio network planning at 3.5 GHz and 28 GHz in a business/dense urban area from the north zone in Quito city, Eng. Proc. (ISSN: 2673-4591) 47 (1) (2023) http: //dx.doi.org/10.3390/engproc2023047024, URL https://www.mdpi.com/2673-4591/47/1/24.
- [11] Yushi Shen, Ed Martinez, Channel estimation in OFDM systems, in: Freescale Semiconductor Application Note, Freescale Semiconductor, Inc. Austian, TX, USA, 2006, pp. 1–15.
- [12] Ayşegül İlay Tunali, Hakan Ali Çirpan, Impact of imperfect channel estimation on 5G-NR, in: 2021 IEEE International Black Sea Conference on Communications and Networking, BlackSeaCom, IEEE, 2021, pp. 1–6.
- [13] Randy Verdecia-Peña, José I. Alonso, A two-hop mmWave MIMO NR-relay nodes to enhance the average system throughput and BER in outdoor-to-indoor environments, Sensors 21 (4) (2021) 1372.
- [14] Jukka-Pekka Nuutinen, Doug Reed, Alfonso Rodriguez-Herrera, 5G MIMO OTA testing on frequency range 2 (FR2), in: 2020 XXXIIIrd General Assembly and Scientific Symposium of the International Union of Radio Science, IEEE, 2020, pp. 1–4.

- [15] Viacheslav Ivanov, Artem Medvedev, Irina Bondareva, Vladimir Grigoriev, Performance of 5G SU-MIMO employing OFDM bandwidth and per-subcarrier precoding, in: Internet of Things, Smart Spaces, and Next Generation Networks and Systems. Springer, 2020, pp. 154–161.
- [16] Hao Qiu, Juan Moreno García-Loygorri, Ke Guan, Danping He, Ziheng Xu, Bo Ai, Marion Berbineau, Emulation of radio technologies for railways: A tapped-delay-line channel model for tunnels, IEEE Access 9 (2021) 1512–1523, http://dx.doi.org/10.1109/ACCESS.2020.3046852.
- [17] Alexandre Matos Pessoa, Bruno Sokal, Carlos F.M.E Silva, Tarcisio Ferreira Maciel, André L.F. De Almeida, Francisco Rodrigo Porto Cavalcanti, A CDLbased channel model with dual-polarized antennas for 5G MIMO systems in Rural Remote Areas, IEEE Access 8 (2020) 163366–163379, http://dx.doi.org/ 10.1109/ACCFSS.2020.3020538.
- [18] Zihao Fu, Hao Cui, Xiongwen Zhao, Yang Wang, Zhihui Wang, Lanxin Qiu, Yanbo Wang, An improved CDL model for 5G millimeter wave communication in a substation scenario, in: 2020 IEEE/CIC International Conference on Communications in China, ICCC Workshops, 2020, pp. 18–22, http://dx.doi.org/10.1109/ICCCWorkshops49972.2020.9209948.
- [19] Imran Khan, Joel JPC Rodrigues, Jalal Al-Muhtadi, Muhammad Irfan Khattak, Yousaf Khan, Farhan Altaf, Seyed Sajad Mirjavadi, Bong Jun Choi, A robust channel estimation scheme for 5G massive MIMO systems, Wirel. Commun. Mob. Comput. 2019 (2019).
- [20] Beixiong Zheng, Changsheng You, Rui Zhang, Efficient channel estimation for double-IRS aided multi-user MIMO system, IEEE Trans. Commun. 69 (6) (2021) 3818–3832, http://dx.doi.org/10.1109/TCOMM.2021.3064947.
- [21] Tobias Lindstrøm Jensen, Elisabeth De Carvalho, An optimal channel estimation scheme for intelligent reflecting surfaces based on a minimum variance unbiased estimator, in: ICASSP 2020 - 2020 IEEE International Conference on Acoustics, Speech and Signal Processing, ICASSP, 2020, pp. 5000–5004, http://dx.doi.org/ 10.1109/ICASSP40776.2020.9053695.
- [22] Ipshita Panda, Sreenath Ramanath, Analysis of beamforming in dense urban deployments, in: 2021 International Conference on COMmunication Systems & NETworkS, COMSNETS, IEEE, 2021, pp. 29–33.
- [23] Anil Agiwal, Mamta Agiwal, Enhanced paging monitoring for 5G and beyond 5G networks, IEEE Access 10 (2022) 27197–27210.
- [24] Mehran Soltani, Vahid Pourahmadi, Ali Mirzaei, Hamid Sheikhzadeh, Deep learning-based channel estimation, IEEE Commun. Lett. 23 (4) (2019) 652–655.
- [25] Eren Balevi, Akash Doshi, Jeffrey G. Andrews, Massive MIMO channel estimation with an untrained deep neural network, IEEE Trans. Wireless Commun. 19 (3) (2020) 2079–2090, http://dx.doi.org/10.1109/TWC.2019.2962474.
- [26] Qiang Hu, Feifei Gao, Hao Zhang, Shi Jin, Geoffrey Ye Li, Deep learning for channel estimation: Interpretation, performance, and comparison, IEEE Trans. Wireless Commun. 20 (4) (2021) 2398–2412, http://dx.doi.org/10.1109/TWC. 2020.3042074
- [27] Mahdi Boloursaz Mashhadi, Deniz Gündüz, Pruning the pilots: Deep learning-based pilot design and channel estimation for MIMO-OFDM systems, IEEE Trans. Wireless Commun. 20 (10) (2021) 6315–6328, http://dx.doi.org/10.1109/TWC. 2021.3073309.
- [28] Pansoo Kim, Sooyeob Jung, Joon-Gyu Ryu, Kyoungpil Ra, Seokhyun Yoon, A study on the development of a modem verification environment for 3GPP NR NTN, in: 2022 International Conference on Electronics, Information, and Communication, ICEIC, IEEE, 2022, pp. 1–2.
- [29] B. Ganesh Kumar, B. S. Kariyappa, Arvind Gupta, Integration and verification of physical layer modules for 5g technology, in: 2019 3rd International Conference on Electronics, Communication and Aerospace Technology, ICECA, 2019, pp. 1214–1219, http://dx.doi.org/10.1109/ICECA.2019.8822003.
- [30] Sassan Ahmadi, 5G NR: Architecture, Technology, Implementation, and Operation of 3GPP New Radio Standards, Academic Press, 2019.
- [31] Erik Dahlman, Stefan Parkvall, Johan Skold, 5G NR: The Next Generation Wireless Access Technology, Academic Press, 2020.
- [32] Xingqin Lin, An overview of 5G advanced evolution in 3GPP release 18, IEEE Commun. Stand. Mag. 6 (3) (2022) 77–83.
- [33] Larry Peterson, Oguz Sunay, Bruce Davie, Private 5G: A Systems Approach, Systems Approach, LLC, 2023.
- [34] Jiyong Pang, Shaobo Wang, Zhenfei Tang, Yanmin Qin, Xiaofeng Tao, Xiaohu You, Jinkang Zhu, A new 5G radio evolution towards 5G-advanced, Sci. China Inf. Sci. 65 (9) (2022) 191301.
- [35] 3rd Generation Partnership Project, 3GPP TS 38.300 version 15.8.0 release 15, 2020
- [36] 3rd Generation Partnership Project, TR 38.321. Medium access control (MAC) protocol specification (release 16), 2022.
- [37] A. Zaidi, F. Athley, J. Medbo, U. Gustavsson, G. Durisi, X. Chen, 5G Physical Layer: Principles, Models and Technology Components, Academic Press, 2018.
- [38] Wan Lei, Anthony C.K. Soong, Liu Jianghua, Wu Yong, Brian Classon, Weimin Xiao, David Mazzarese, Zhao Yang, Tony Saboorian, 5G System Design And End to End Perspective, SpringerLink, 2020.
- [39] 3rd Generation Partnership Project, TR 38.827. Study on radiated metrics and test methodology for the verification of multi-antenna reception performance of NR user equipment (UE); (release 16), 2022.

- [40] 3rd Generation Partnership Project, TR 138.900. Study on channel model for frequency spectrum above 6 GHz, 2022.
- [41] 3rd Generation Partnership Project, TR 138.901. Study on channel model for frequencies from 0.5 to 100 GHz, 2022.
- [42] Marcus V.G. Ferreira, Flávio Henrique Teles Vieira, Delay minimization based uplink resource allocation for device-to-device communications considering mmwave propagation, PeerJ Comput. Sci. 7 (2021) e462.
- [43] MATLAB, 5G Toolbox, 2021, URL https://la.mathworks.com/products/5g.html.
- [44] Gordana-Raluca Barb, Marius Otesteanu, Georgeta Budura, Cornel Balint, Performance evaluation of TDL channels for downlink 5G MIMO systems, in: 2019 International Symposium on Signals, Circuits and Systems, ISSCS, IEEE, 2019, pp. 1–4.
- [45] 3rd Generation Partnership Project, TR 38.901. Study on channel model for frequencies from 0.5 to 100 GHz (release 16), 2022.
- [46] Chang-Jae Chun, Jae-Mo Kang, Il-Min Kim, Deep learning-based channel estimation for massive MIMO systems, IEEE Wirel. Commun. Lett. 8 (4) (2019) 1228–1231.
- [47] Mahdi Boloursaz Mashhadi, Deniz Gündüz, Pruning the pilots: Deep learningbased pilot design and channel estimation for MIMO-OFDM systems, IEEE Trans. Wireless Commun. 20 (10) (2021) 6315–6328.
- [48] Hao Ye, Geoffrey Ye Li, Biing-Hwang Juang, Power of deep learning for channel estimation and signal detection in OFDM systems, IEEE Wirel. Commun. Lett. 7 (1) (2017) 114–117.
- [49] Jo Schlemper, Jose Caballero, Joseph V Hajnal, Anthony Price, Daniel Rueckert, A deep cascade of convolutional neural networks for MR image reconstruction, in: Information Processing in Medical Imaging: 25th International Conference, IPMI 2017, Boone, NC, USA, June 25-30, 2017, Proceedings 25, Springer, 2017, pp. 647–658.
- [50] Rémi Cresson, Nicolas Narçon, Raffaele Gaetano, Aurore Dupuis, Yannick Tanguy, Stéphane May, Benjamin Commandre, Comparison of convolutional neural networks for cloudy optical images reconstruction from single or multitemporal joint SAR and optical images, 2022, arXiv preprint arXiv:2204.00424.
- [51] Keiron O'shea, Ryan Nash, An introduction to convolutional neural networks, 2015, arXiv preprint arXiv:1511.08458.
- [52] Divya Arora, Mehak Garg, Megha Gupta, Diving deep in deep convolutional neural network, in: 2020 2nd International Conference on Advances in Computing, Communication Control and Networking, ICACCCN, IEEE, 2020, pp. 749–751.
- [53] 3rd Generation Partnership Project, TR 38.913. Study on scenarios and requirements for next generation access technologies: (release 17), 2022.
- [54] 3rd Generation Partnership Project, 3GPP TS 38.101 version 17.12.0 release 17, 2024
- [55] Chao Dong, Chen Change Loy, Kaiming He, Xiaoou Tang, Image super-resolution using deep convolutional networks, IEEE Trans. Pattern Anal. Mach. Intell. 38 (2) (2015) 295–307.



Juan Diego Belesaca received a bachelor's degree in Electronics and Telecommunications, a Master's degree in Strategic Management of Information Technologies, and a Master of Science degree in Electrical Engineering Sciences (Honors) specializing in mobile communications, all from the University of Cuenca in 2018, 2021, and 2024, respectively. He has four years of experience as a researcher at the Department of Electrical Engineering, Electronics, and Telecommunications (DEET) at the same university. Juan Diego focuses on studying and developing advanced technologies in mobile communications, significantly contributing to academic research in his field.



Andres Vazquez-Rodas received the Electronics Engineering degree in 2004 from the Universidad Politécnica Salesiana Cuenca – Ecuador, the Master degree in Telematics Engineering (Honors) from the Universidad de Cuenca – Ecuador in 2010, and the Ph.D. from the Networking Department of the Universitat Politècnica de Catalunya BarcelonaTech (UPC), Spain in 2015. He was also a professor at the Universidad Politécnica Salesiana until 2017. Since 2015 he is full time professor of the Universidad de Cuenca at the Electric, Electronic and Telecommunication Department (DEET) and the Engineering Faculty. His research interests include wireless mesh networks, mobile networks, wireless sensor networks, industrial networking and complex systems.



Luis F. Urquiza-Aguiar received the M.Sc. and Ph.D. degrees in Telematics Engineering and the M.Sc. degree in Statistics and operational research from the Universitat Politècnica de Catalunya, Barcelona, Spain, in 2012, 2016, and 2018, respectively. He is currently an Associate Professor with the Departamento de Electrónica, Telecomunicaciones y Redes de Información, Escuela Politécnica Nacional (EPN), Quito, Ecuador.He is a Coordinator of Grupo de Investigación en Redes Inalámbricas (GIRI), which was awarded among best research groups from EPN in 2019 and 2021. He has authored more than 50 conference and journal publications on performance evaluation of adhoc wireless networks, vehicular networks, and 5G. He was the recipient of the MSWiM'21 RISING STAR Award. His research interests include wireless networks, mathematical modeling, and the optimization of large-scale telecommunication problems. He holds the Associate Level Researcher accreditation from SENESCYT, Ecuador.



José David Vega Sánchez (Member, IEEE) received the B.Sc. degree in electronics engineering from Escuela Politécnica del Ejército (ESPE), Sangolquí, Ecuador, in 2013, the M.Sc. degree in electrical engineering from the University of Campinas (UNICAMP), São Paulo, Brazil, in 2015, and the Ph.D. degree in electrical engineering from Escuela Politécnica Nacional (EPN), Quito, Ecuador, in 2022. He was a Visiting Researcher with the University of Málaga, Spain, in 2023. He is currently a member of the Grupo de Investigación en Redes Inalámbricas (GIRI), awarded among the best research groups from EPN, in 2019 and 2021. His research interests include modeling, analysis, and the simulation of wireless fading channels.